D3.3 – Corrosion test results of the selected coatings

Project information

Project title	Advanced Processes Enabling Low cost and High Performing Large Scale Solid Oxide Electrolyser Production
Project acronym	PilotSOEL
Start date	01-06-2023
Type of action	HORIZON-JU-RIA
GA number	101112026
Duration	36 months
Project website	www.pilotSOEL.dtu.dk

Deliverable information

Deliverable number	*D3.3*
Deliverable title	*Corrosion test results of the selected coatings*
WP number	*WP3*
WP title	*Advanced surface coating technologies for IC plate*
WP leader	*NACO*
Responsible partner	*ELCOY*
Contributing partners	*NACO*
Authors	*Jouni Puranen, Luiza Souza*
Contributors	*Janis Zideluns*
Deliverable type	*R*
Dissemination level	*PU*
Contractual deadline	*31-01-2025*
Delivery date to EC	*30-01-2025*

Co-funded by the European Union

Clean Hydrogen Partnership

The project is supported by the Clean Hydrogen Partnership and its members. Views and opinions expressed are however those of the author(s) only and do not necessarily reflect those of the European Union or the Clean Hydrogen Partnership. Neither the European Union nor the Clean Hydrogen Partnership can be held responsible for them.

1. Content

2. Introduction

Interconnectors in solid oxide electrolysers (SOEL) are typically manufactured using ferritic stainless steels with a chromium content of 18–22 wt-%. This composition allows the steel to form a protective Cr-rich oxide scale, typically Cr_2O_3, at elevated temperatures. However, under certain conditions and in the presence of water vapor, the scale can form volatile hydroxide compounds, such as $CrO_2(OH)_2$ and $CrO_2(OH)$. These hydroxides are transported to the active air electrode, where they form (Sr,Cr)-oxide compounds, causing Cr-poisoning and leading to degradation. Additionally, the formation of Cr-rich scales increases ohmic resistance, which directly impacts stack performance.

To prevent degradation and performance issues, interconnects are coated with ceramic-based protective coatings. These coatings act as a barrier, preventing Cr_2O_3 from reacting with water vapor to form volatile species. They also reduce the growth rate of Cr-rich scales, enabling improving stack performance and extending operational lifetime.

One of the objectives of the PilotSOEL project is to identify cobalt-free coating candidates to replace commonly used manganese-cobalt spinels. Cobalt is classified as a critical raw material (CRM) and is known for its carcinogenic properties. A wide range of coating candidates was reviewed in Deliverable 3.1: List of coating candidates for air and fuel sides of interconnect plates, based on scientific literature related to solid oxide fuel cell and electrolyser technologies. Four candidates were selected for further study using various ex-situ methods that simulate actual stack operating conditions. At least one of these coatings should meet the key performance indicators (KPIs) set for this project by achieving an ASR value lower than 5 $m\Omega*cm^2$ after 3000 hours of operation.

3. Materials and methods

3.1 Selected coatings

The coatings (Table 1) discussed in this deliverable were manufactured using the Naco 600 magnetron sputter, which is a physical vapor deposition (PVD) method. Parameter optimization was performed and reported in Deliverable 3.2: Optimal coating compositions and deposition parameters for the air and fuel side. Each coating was deposited on Crofer 22 APU (VDM Metals), a ferritic stainless steel (FSS) plate with a thickness of 0.3 mm. Only surface cleaning was performed as the pre-treatment process, using organic solvents followed by rinsing with deionized water. Although the project focuses on cobalt-free or cobalt-reduced candidates, $(Mn,Co)_3O_4$ was selected as a reference material due to the extensive research data available on this coating composition.

Table 1. Selected coating for corrosion tests

Coating	Thickness (nm)	Note
Mn_2CuO_4	1250 nm	
$Mn_{1.5}Cu_{1.5}O_4$	1120 nm	
$Mn_{1.5}Cu_{0.75}Co_{0.7}O_4$	1230 nm	
$Mn_{1.5}Co_{1.5}O_4$	850 nm	Reference coating

As-received and oxidized samples were analyzed using field-emission scanning electron microscopy (FE-SEM) with a Tescan Clara. Standard sample preparation methods were applied prior to analysis, including casting samples in cold epoxy, cutting, and polishing the cross-section surface. The coating cross-sections and topographies are shown in Figure 1. As expected, the coating exhibited a dense microstructure, which is typical for coatings produced using the PVD technique. A dense microstructure is beneficial for protective coatings, as it helps prevent volatile compounds from transferring from the substrate to the active oxygen electrode. Since the coating thicknesses were approximately 1.5 µm or less, the surface topography images also reveal the substrate's topography, displaying typical features formed during hot and cold rolling, such as rolling lines and fatigue-related surface damage.

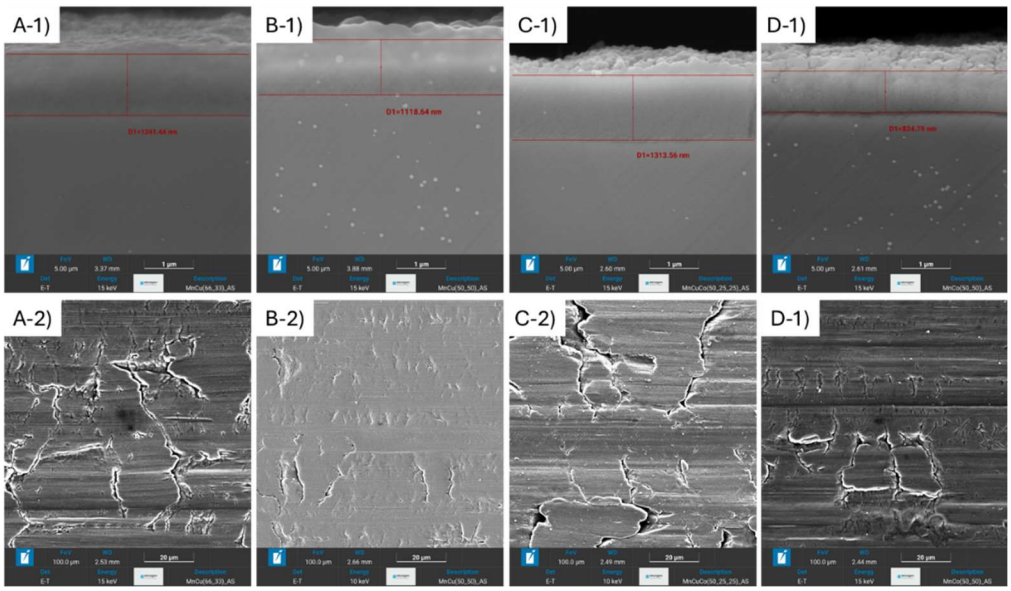

Figure 1. As-received PVD coatings cross-sections (top row) and topography (bottom row) SEM images of a) Mn_2CuO_4, b) $Mn_{1.5}Cu_{1.5}O_4$ c) $Mn_{1.5}Cu_{0.75}Co_{0.75}O_4$ and d) $Mn_{1.5}Co_{1.5}O_4$ coatings.

3.2 Area specific resistance

Area specific resistance (ASR) measurements were conducted to evaluate how metals combined with various coatings conduct electricity at elevated temperatures, particularly when oxide scales form between the metal substrate and the protective coatings. The ASR measurement setup is based on the four-point measurement method, in which a known current is passed through a set of coated samples, and the voltage drop is recorded. Using the known current, voltage, and sample area, the ASR value is calculated and compared across samples with different coatings. The lower and more stable the ASR during long-term operation, the better the material system performs.

Elcogen Oy has developed its own ASR test setup (Figure 2), capable of measuring up to 75 double-sided coated samples simultaneously, stacked together without any contact paste. In the test bench, surface compression forces (0.2–5 MPa), current densities (0.1–3 A/cm^2), and temperatures (500–800 °C) can be adjusted to simulate real stack conditions. This active compression enables measurements without contact pastes, improving reliability. To further enhance accuracy, each metal-coating variant includes five separate measurements, resulting in four ASR values. To account for the sample size, the total area represented by the measurements is approximately 60 cm^2. In the PilotSOEL project, ASR measurements were conducted at two different temperatures. First, samples were tested for 3200 hours at 650 °C. After completion, the temperature was increased to 700 °C, and testing continued for another 1650 hours. This test setup provided a better understanding of how different coatings protect against oxidation under varying operating conditions.

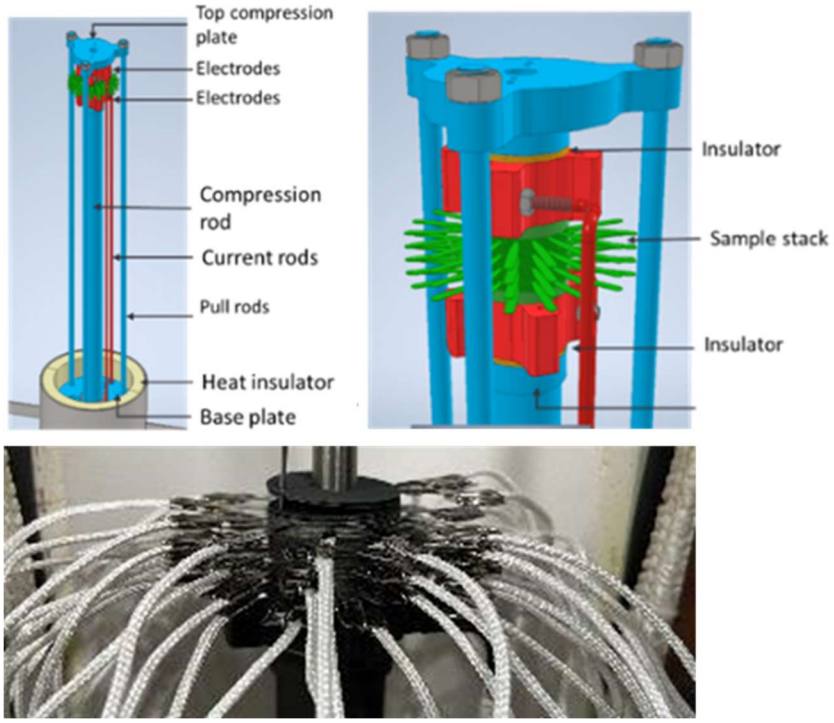

Figure 2. Elcogen Oy in-house built ASR test bench

3.3 Single and dual atmosphere oxidation

Single-atmosphere (SA) and dual-atmosphere (DA) tests are straightforward methods for evaluating how well applied coatings protect steel in different gas environments. Under SA conditions, the sample is placed inside a muffle furnace with a stagnated air atmosphere. A temperature of 650 °C was selected for this test, as it corresponds to the temperature used in ASR testing. This test simulates the oxidation of components used exclusively on the anode side of the SOEL stack, for example various contact structures. Additionally, cross-section data collected from these samples can help explain ASR anomalies. For example, if ASR values increase rapidly and cross-section analysis reveals a high growth rate of oxide scales between the metal and the protective coatings, it may indicate degradation for that material system.

The DA test (Figure 3) is conducted by exposing one side of the sample to oxidizing conditions and the other side to reducing conditions. The purpose of this test is to simulate the conditions that an interconnector experiences during stack operation. Elcogen OY has built its own dual-atmosphere test bench, which can hold up to 36 samples. It operates by exposing one side of the sample to air and the other side to 5% formier gas. The temperature can be adjusted between 500 and 800 °C to simulate various operating conditions. The gas flow rate on the fuel side is controlled, while the air side remains stagnant.

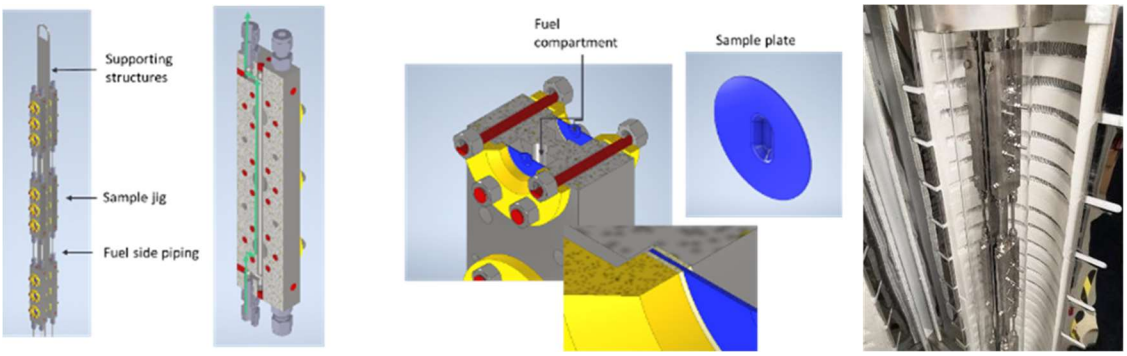

Figure 3. Elcogen Oy's dual atmosphere test jig

The test was conducted at 600 and 700 °C. This relatively low temperature range was chosen because it poses a challenge for the FSS components due to the lower diffusion rate of alloying elements. Due to limited diffusion, FSS is more susceptible to breakaway oxidation, a phenomenon that can lead to the failure of solid oxide stacks. Higher temperatures more accurately represent real stack conditions when operating in electrolysis mode.

4. Results and discussion

4.1 Area specific resistance

Stack performance is closely related to the electrical conductivity of interfaces. One of the critical interfaces is the contact between the cell and the interconnector, which is significantly influenced by the thickness of oxide layers formed during operation. ASR measurements enable the evaluation of oxide layer growth kinetics and conductivity, as well as the effectiveness of protective coatings in reducing their growth rate. Figure 4 presents the ASR values measured for the coatings selected for testing.

The first test was conducted at 650 °C for 3200 hours, with all samples tested simultaneously. According to the results, none of the coatings exceeded the 5 mΩ*cm² threshold defined as one of the KPIs for the PilotSOEL project. One of the best-performing coatings was $Mn_{1.5}Cu_{1.5}O_4$. This finding aligns with literature, as Mn-Cu spinels typically exhibit the highest electrical conductivities (up to 120 S/cm) at these temperatures, as also noted in Deliverable 3.1. This is more than double the conductivity of $(Mn,Co)_3O_4$ spinels. The lowest performance was observed for $(Mn,Co,Cu)_3O_4$. However, it should be noted that the 2.5 mΩ*cm² difference between the best- and lowest-performing coatings could also result from measurement system inaccuracies or small surface defects, which may alter the contact area and, consequently, affect the results.

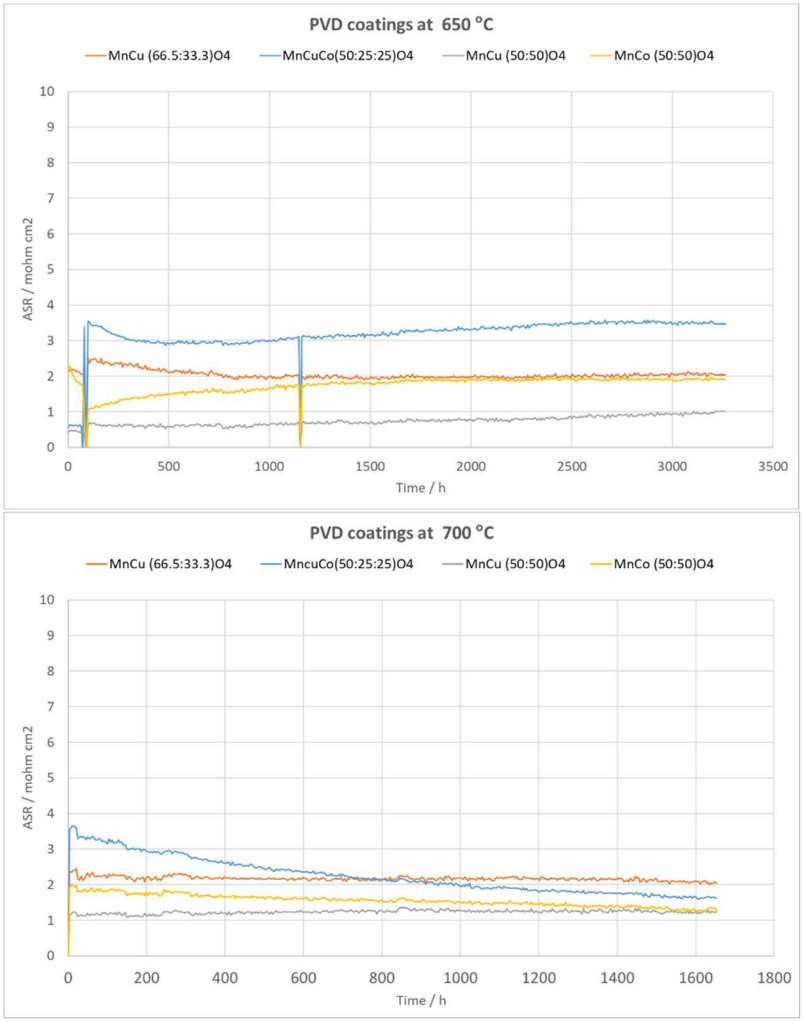

Figure 4. ASR test results obtained at 650 °C (top) and 700 °C (bottom)

To have a better understanding of how coating-metal interfaces behave under various conditions, the test temperature was increased to 700 °C. This temperature also represents the SOEL stack's middle and outlet temperatures, making it equally important to evaluate material performance in this range, as electrochemical reactions occur also in the active outlet areas.

The increase in temperature resulted in a decrease in ASR values for $(Mn,Co,Cu)_3O_4$ and $(Mn,Co)_3O_4$, whereas the rest of the coatings maintained a relatively stable performance compared to their operation at 650 °C. This outcome was expected, as the protective coatings and Cr-oxide scales formed between the metal substrate and the protective coatings are p-type semiconductors, meaning that increasing temperature reduces resistivity. The stable performance of the coatings during ASR testing at both temperatures indicates that they effectively limit excessive growth of the Cr-rich oxide scale between the substrate and the protective coatings. If the layers were to fail and the oxide scale continued to grow extensively, this would be observed as a continuous increase in the ASR value.

4.2 Single atmosphere oxidation

The coated samples were oxidized under single-atmosphere conditions at 650 °C for 2000 hours to evaluate how effectively the protective coatings prevent oxide scale growth. The cross-section images of the coatings oxidized for 2000 hours are presented in Figure 5. According to the cross-section data, $(Mn,Cu)_3O_4$ exhibits the so-called breakaway oxidation phenomenon, meaning that the formed oxide layer grows unevenly toward the metal substrate. Elemental analysis using energy-dispersive spectroscopy (EDS) shows that the breakaway oxidation blisters consist of multiple phases. A Cr-rich oxide layer grows inward toward the metal, while an Fe-rich layer extends outward from the substrate surface. The oxide layer growth occurs beneath the protective coatings, as higher concentrations of Mn and Cu were observed on top of the blister, with thicknesses similar to the as-received layer.

The highest level of protectiveness was observed with $Mn_{1.5}Cu_{0.75}Co_{0.75}O_4$ and $Mn_{1.5}Co_{1.5}O_4$ coatings. The cross-sections show only minor blister formation, and overall, the coatings exhibit a microstructure similar to the as-received condition. The densest microstructure was achieved with $Mn_{1.5}Co_{1.5}O_4$, while $Mn_{1.5}Cu_{0.75}Co_{0.75}O_4$ showed a slightly more porous structure. Both coatings had a homogeneous elemental composition, with a slight increase in Cr intensity observed at the interface between the substrate and the protective coating, indicating the formation of a Cr-rich oxide layer

Interestingly, $(Mn,Cu)_3O_4$-based coatings provided the lowest ASR values, which suggests that oxide scale growth should be minimal, if present at all. However, when the samples were freely oxidized, they exhibited a strong tendency to oxidize. One possible explanation is that during ASR testing, oxygen availability is limited. This could be due to the test setup, where samples face each other without a porous contact paste layer that would facilitate better oxygen diffusion to the mating surfaces, thereby restricting oxide scale growth. This hypothesis will be confirmed when the test arrangement is disassembled, as the test was still ongoing when Deliverable 3.3 was reported.

The improved conductivity of $Mn_{1.5}Cu_{0.75}Co_{0.75}O_4$, observed as the largest drop in ASR during testing when the temperature was increased, could be explained by the presence of a thicker Cr-rich oxide scale compared to the other tested samples. The thickness of the Cr-rich layer can be evaluated by comparing the EDS map of Cr intensity against that of $Mn_{1.5}Co_{1.5}O_4$ samples.

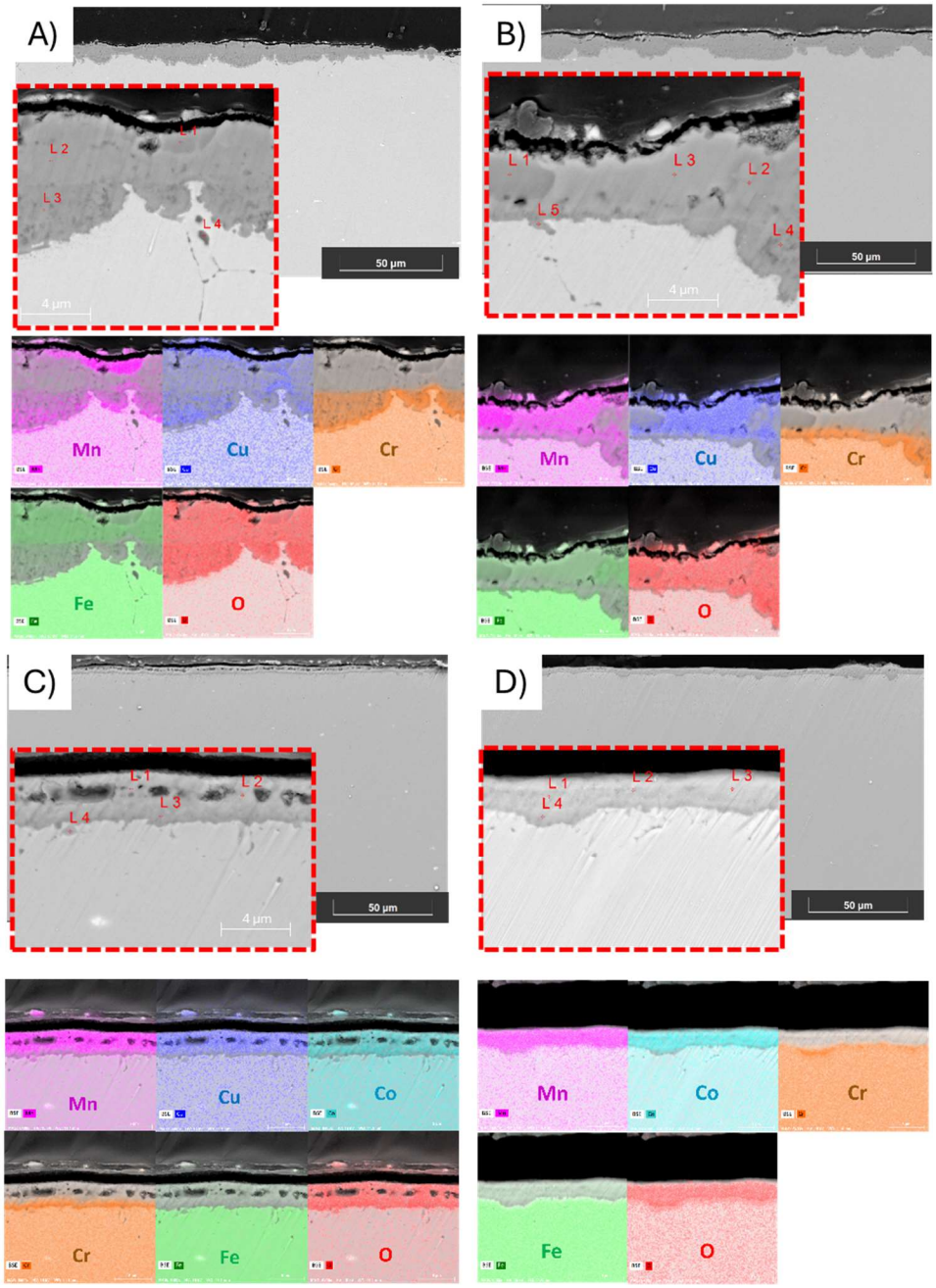

Figure 5. SEM cross-section images of a) Mn_2CuO_4, b) $Mn_{1.5}Cu_{1.5}O_4$ c) $Mn_{1.5}Cu_{0.75}Co_{0.75}O_4$ and d) $Mn_{1.5}Co_{1.5}O_4$ coatings oxidized for 2000 hours at 650 °C.

In addition to cross-section images, surface analyses were conducted to examine topographical differences between the coatings. These SEM topography images, along with EDS area mapping, are shown in Figure 6 and EDS mapping in Figure 7. The strong oxidation observed in the $(Mn,Cu)_3O_4$-based spinels in the cross-section images was also evident in the topographical analysis. The most pronounced oxidation occurred in the Mn_2CuO_4 coating, confirmed by blister

formation with a higher Fe concentration according to EDS analysis. Similar Fe-rich areas were also detected in $Mn_{1.5}Cu_{1.5}O_4$ coatings, though with slightly smoother surface roughness.

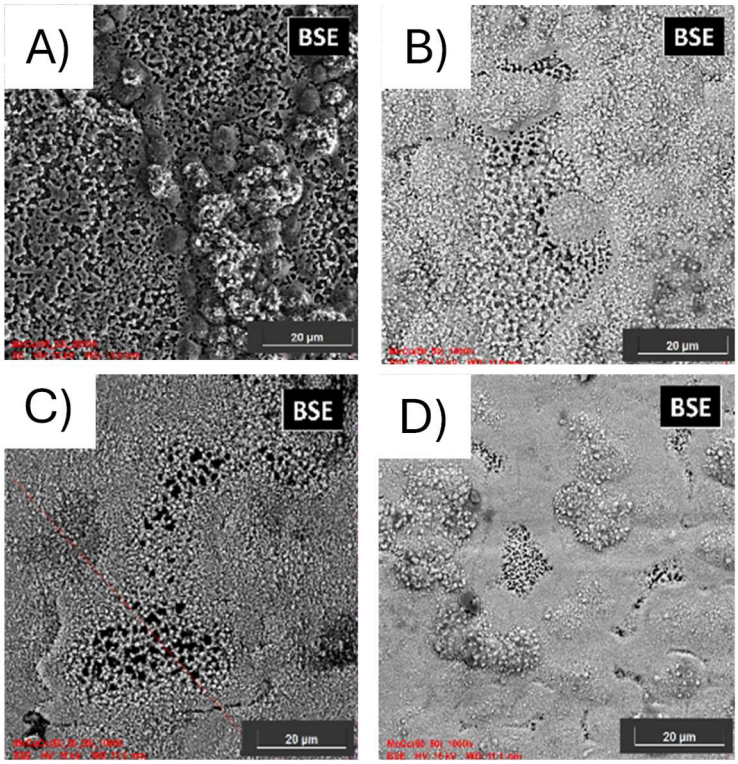

Figure 6. SEM topography images of a) Mn_2CuO_4, b) $Mn_{1.5}Cu_{1.5}O_4$ c) $Mn_{1.5}Cu_{0.75}Co_{0.75}O_4$ and d) $Mn_{1.5}Co_{1.5}O_4$ coatings oxidized for 2000 hours at 650 °C.

Depending on the stack design, the interconnector surface on the anode side is partially exposed to the air atmosphere and partially in contact with components such as the current collector mesh or the oxygen electrode. There is a clear risk that areas not in direct contact with other surfaces may release Cr species, which can gradually accumulate on the oxygen electrode and cause Cr poisoning.

Cobalt-containing coatings also exhibited increased porosity in the topographical analysis. The EDS maps showed a fairly homogeneous composition, even in more porous areas. It is possible that these porous regions are connected to the metal surface, particularly in locations where the as-received coatings indicate that the substrate may have fatigue-related surface damage due to hot and cold rolling. These areas might limit the diffusion of alloying elements, potentially leading to stronger oxidation.

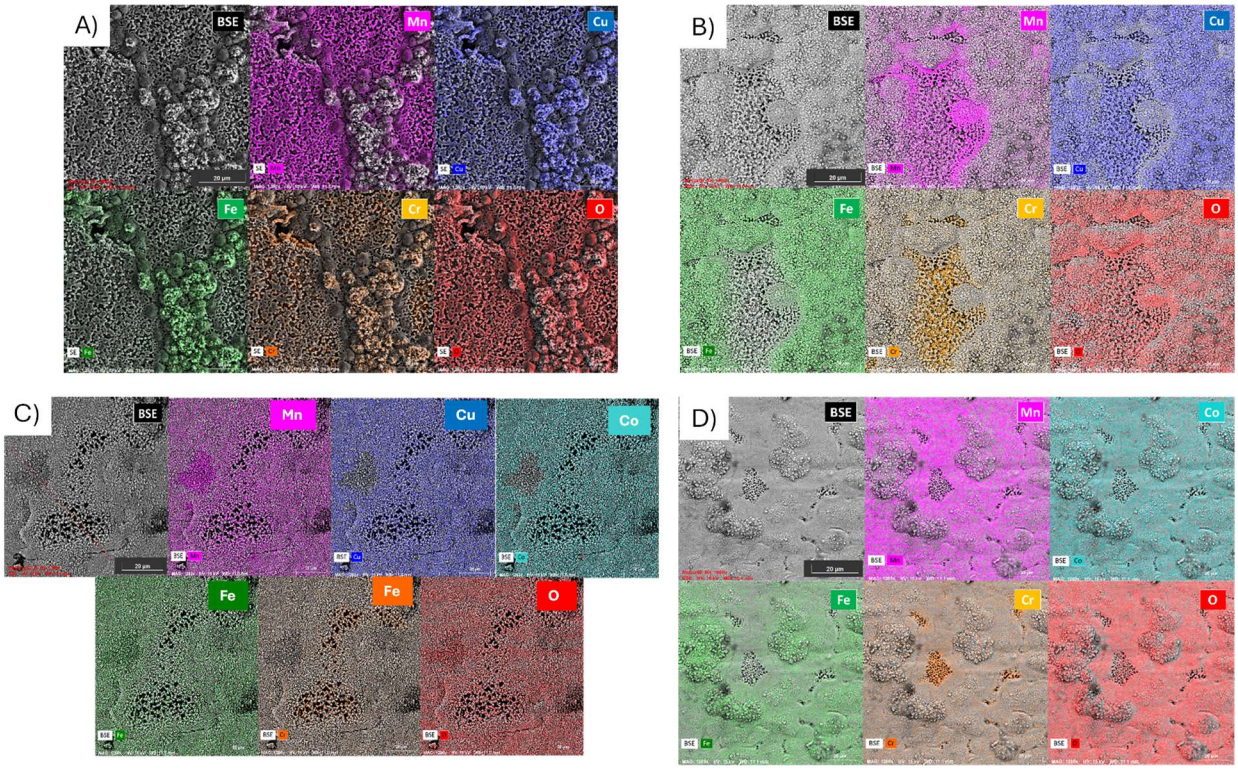

Figure 7. SEM topography images with EDS mapping of a) Mn_2CuO_4, b) $Mn_{1.5}Cu_{1.5}O_4$ c) $Mn_{1.5}Cu_{0.75}Co_{0.75}O_4$ and d) $Mn_{1.5}Co_{1.5}O_4$ coatings oxidized for 2000 hours at 650 °C.

4.3 Dual atmosphere oxidation

Since the primary purpose of protective coatings is to prevent the interconnect from oxidation, it is important to understand how well they provide corrosion protection under dual-atmosphere conditions. This was tested by placing two sets of coated samples in the same furnace, with one temperature zone set to 600 °C and the other to 700 °C. The same forming gas was used to flush the fuel side of the samples. The cross-section images of these coatings are shown in Figures 8 and 9.

All coating candidates experienced some level of breakaway oxidation. The microstructure and elemental composition of individual blisters appeared similar to those observed in samples oxidized under single-atmosphere conditions: a Cr-rich oxide grew inward toward the metal, while an Fe-rich oxide extended outward from the substrate. Typically, 600 °C is considered more challenging for FSS due to the limited diffusion rate of alloying elements. However, in this case, the outcome appears to be comparable, regardless of whether the sample was oxidized at 600 °C or 700 °C.

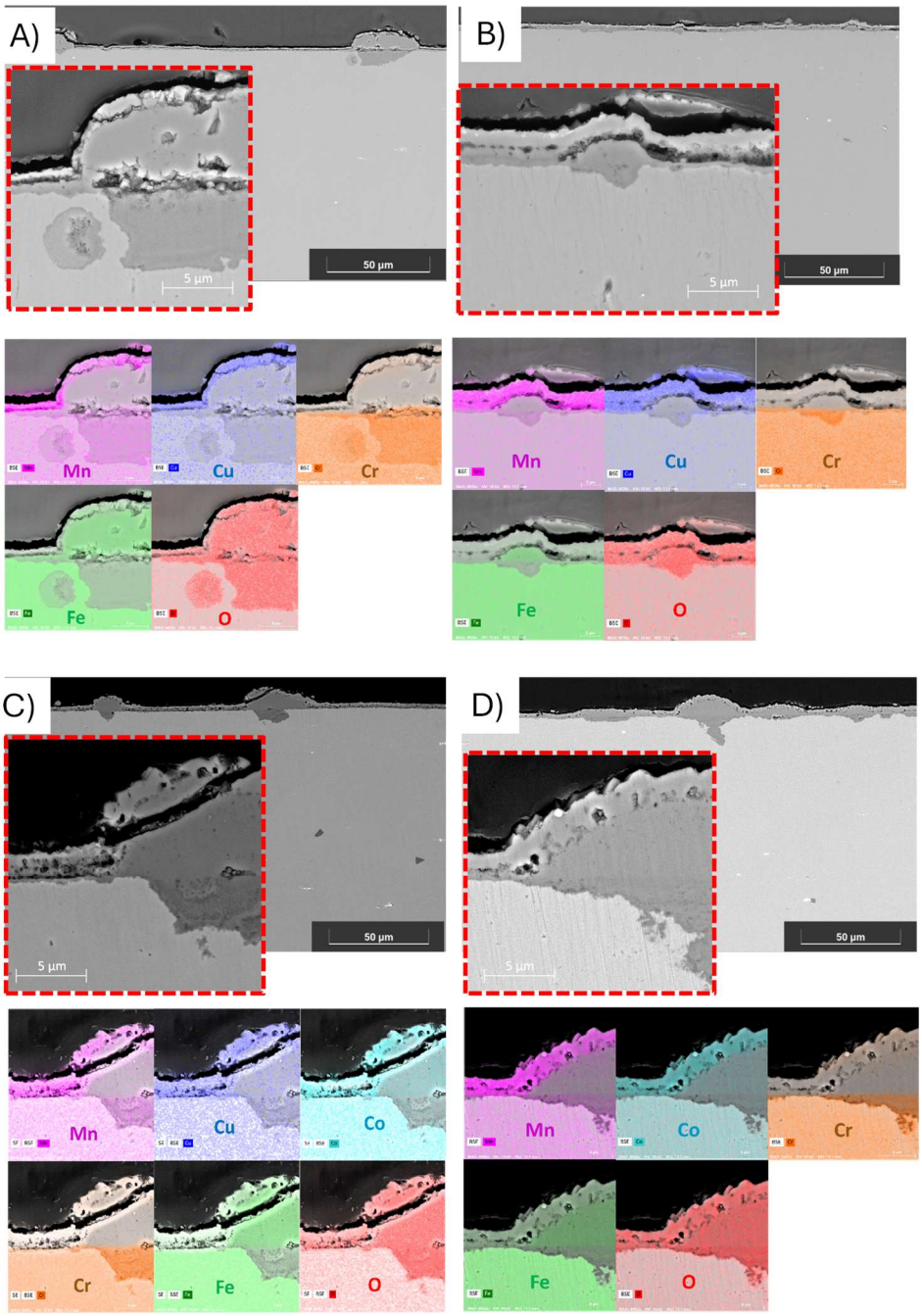

Figure 8. SEM cross-sections images of a) Mn_2CuO_4, b) $Mn_{1.5}Cu_{1.5}O_4$ c) $Mn_{1.5}Cu_{0.75}Co_{0.75}O_4$ and d) $Mn_{1.5}Co_{1.5}O_4$ coatings oxidized for 1000 hours at 600 °C.

In these tests, the best-performing coating was the reference $Mn_{1.5}Co_{1.5}O_4$, which showed no breakaway oxidation at 700 °C. The completely cobalt-free candidates exhibited a relatively thick oxide layer at 700 °C, whereas the cobalt-less variant, $Mn_{1.5}Cu_{0.75}Co_{0.75}O_4$, displayed a

heterogeneous oxide layer thickness and composition. Some areas were not heavily oxidized, while others had an oxide layer of similar thickness to that of $(Mn,Cu)_3O_4$ spinels.

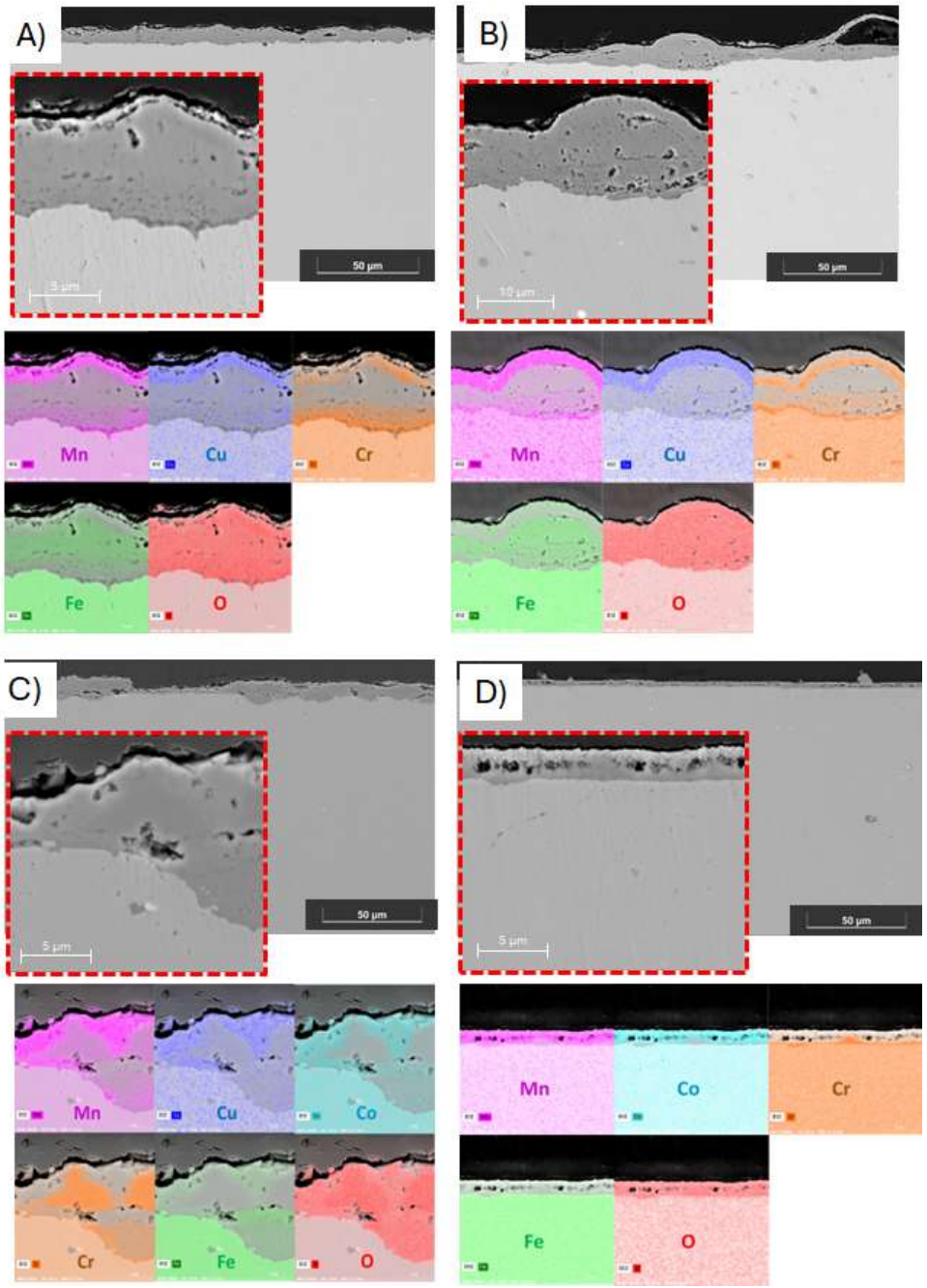

Figure 9. SEM cross-sections images of a) Mn_2CuO_4, b) $Mn_{1.5}Cu_{1.5}O_4$ c) $Mn_{1.5}Cu_{0.75}Co_{0.75}O_4$ and d) $Mn_{1.5}Co_{1.5}O_4$ coatings oxidized for 1000 hours at 700 °C.

5. Conclusion

Four different coatings: i) Mn_2CuO_4, ii) $Mn_{1.5}Cu_{1.5}O_4$, iii) $Mn_{1.5}Cu_{0.75}Co_{0.75}O_4$, and iv) $Mn_{1.5}Co_{1.5}O_4$ were tested in various ex-situ experiments to evaluate their ability to prevent interconnect oxidation and provide low ohmic resistance, thereby enhancing stack performance in electrolysis mode. The ASR and single-atmosphere oxidation tests were conducted at 650 °C in an air atmosphere. ASR testing was also continued at 700 °C to gain a better understanding of oxidation kinetics and the electrical performance of the protective coatings. Additionally, dual-atmosphere tests were conducted at 600 and 700 °C. The lower temperature was selected because it is known to be problematic for FSS due to the limited diffusion of alloying elements, which makes uncontrolled oxidation more likely. The higher temperature was chosen as it closely reflects the average operating temperature of the electrolyser stack.

According to various ex-situ tests, the most suitable candidate for the air-side coating is $Mn_{1.5}Cu_{0.75}Co_{0.75}O_4$. This coating initially exhibited the highest ASR values at lower temperatures, but when the test temperature was increased to 700 °C, its electrical performance matched with other coating candidates. $Mn_{1.5}Cu_{0.75}Co_{0.75}O_4$ was the only coating composition that did not show any signs of breakaway oxidation under single-atmosphere conditions, whereas other cobalt-free candidates failed, showing a strong tendency for breakaway oxidation. A small number of breakaway blisters were observed under dual-atmosphere conditions, but the amount was comparable to that of other tested coating variants.